

Multi-temporal remote sensing data and spectral indices analysis for detection tropical rainforest degradation: case study in Kapuas Hulu and Sintang districts, West Kalimantan, Indonesia

Parwati Sofan¹ · Yenni Vetrita¹ · Fajar Yulianto¹ ·
Muhammad Rokhis Khomarudin¹

Received: 1 July 2014 / Accepted: 10 October 2015 / Published online: 27 October 2015
© Springer Science+Business Media Dordrecht 2015

Abstract According to the forest statistic data, the forest degradation in West Kalimantan has been increasing since 2006. The satellite remote sensing data can provide information more effective and economical input rather than direct field observation that is difficult to access. In this research, we applied a spectral index derived from remote sensing satellite data, the Normalized Difference Fraction Index (NDFI), then compared it with the widely used forest degradation index, the Normalized Burn Ratio (NBR) and the Normalized Difference Vegetation Index (NDVI), in order to have an enhanced detection of forest canopy damage caused by selective logging activities and associated forest fires in West Kalimantan, especially in Kapuas Hulu and Sintang districts. The NDFI was derived from combination of green vegetation, shadow, soil, and non-photosynthetic vegetation (NPV) fractions images from spectral mixture analysis model. The NBR and NDVI were generated from spectral reflectance values of near-infrared, shortwave infrared, and red spectrums. The satellite data used for monitoring forest degradation were Landsat-year 2006–2009 and then continued with 4-year SPOT 2009–2012. The result showed that the forest degradation was detected initially in 2008 up to 2012 in the research area. Spectral indices analysis (NDFI, NBR, NDVI) was tested and verified by ground survey data in 2012. We found that NDFI has higher accuracy (95 %) to classify the degradation forest due to logging and burning activities rather than NBR or NDVI. The forest degradation mapping also conducted using mosaic of Landsat data year 2000–2009 for whole of West Kalimantan province. This method is suitable for a forest degradation monitoring tool in tropical rainforest.

Keywords Forest degradation · NDFI · NBR/NDVI · SPOT-4 · Landsat · West Kalimantan · Indonesia

✉ Parwati Sofan
parwati@lapan.go.id

¹ Remote Sensing Applications Center, Indonesian National Institute of Aeronautics and Space (LAPAN), Jl. Kalisari No. 8, Pekayon, Pasar Rebo, Jakarta Timur 13710, Indonesia

1 Introduction

Tropical rainforest in Indonesia is one of the very precious natural resources to the world. Tropical rainforest is known as the “lungs of the planet” containing a rich variety of flora and fauna, which helps to counter weight global warming which occurs in the recent decade (Cox et al. 2013). The area of Indonesian forest in 2012 reached 130.61 million hectares, contributing 68.6 % of the total land area to become one of the natural resource potential which is vulnerable to damage due to human activities in meeting their needs (Ministry of Forestry 2012).

The rate of deforestation and forest degradation in Indonesia between 1998 and 2002 reached 1.1 million per year or equivalent to approximately 3.5 million hectares (Ministry of Forestry 2013). Meanwhile, according to Indonesian forestry statistics in 2011 (Ministry of Forestry 2012), the area of critical land in Indonesia was 27.3 million ha, of which reflects land degradation that was damaged due to vegetation loss, resulting in reduced forest functionality as water reservoir, erosion control, nutrient cycles, micro-climate regulator, and carbon retention. There are three provinces with the largest critical land in Indonesia between 2006 and 2011. These area are Central Kalimantan (4.6 million ha), South Sumatra (3.9 million ha), and West Kalimantan (3.2 million ha). With regard to the above findings, observations on forest condition and forest status need to be done in order to maintain its condition, to provide an input for forest management and forest/land damaged handling.

Forest degradation is different to deforestation. In order to demonstrate and understand the difference between these two phenomena, meaning and definition of forest should initially be well understood. Bajracharya (2008) has conducted a study based on several literatures, expert meetings and laymen assumptions to obtain comprehensive definition of forest degradation. Forest degradation is concluded as canopy cover change and decline in biodiversity caused by human activities such as logging and forest fires that lowers carbon stocks and forest productivity in the long run. Selective logging is a form of timber extraction on a group of trees in the forest, in which tree species have been selected because of its economic benefits. Selective logging is usually located in a natural forest where there are access roads and logging tracks. In selective logging, at least about 10–46 % of living biomass is harmed or died during harvesting season (Veríssimo et al. 1992, 1995; Nepstad et al. 1999; Gerwing 2002). Selective logging damages a land area of 1503–2275 m²/ha (Johns et al. 1996), so that the forest canopy will be reduced by approximately 40–50 % of the original condition (Veríssimo et al. 1992; Gerwing 2002). The other man activities that caused forest degradation is forest fire which usually performed by humans after opening the forest through logging. Forest fire can be deadly to more than 98 % of trees with a diameter greater than 20 cm, and leave living trees of 10–40 % of the forest canopy (Cochrane et al. 1999). Many studies have confirmed the definition of deforestation as the non-temporal change from forest use to others landuse, whereas forest degradation is the decline in forest quality (Turner II et al. 1993; Verolme and Moussa 1999; Lanly 2003).

Utilization of remote sensing data to identify forest degradation due to selective logging and forest fires has been developed by researchers in mapping the degradation. Visual classification in the era of 2000 is the first technique performed for forest cover monitoring and selective logging (Achard and Hansen 2012). However, visual interpretation can be done when trace of logged area is visible on the satellite image data. In general, the trace of logged area will appear one or 2 years after the actual logging. Visual classification is more time-consuming and has potential bias/error during data interpretation. Furthermore, digital image processing techniques such as the minimum distance and maximum likelihood have been developed and utilized to map selective logging practice, as was done by Stone and Lefebvre

(1998), Roberts et al. (1998) and Shimabukuro et al. (1998). The use of such techniques is prone to errors due to value similarity between selective logging areas with various different vegetation age and intensity of logging, as well as natural forests. In degraded forest, several other phenomenon and objects coexist such as forest regeneration, dead vegetation, and open land, resulting in greater difficulty for satellite data identification (Souza et al. 2003).

Analysis of forest degradation mainly caused by forest fires have been frequently made through remote sensing satellite data collection, with the use of satellite remote sensing in low-to-medium spatial resolution such as: MODIS (Martín et al. 2002; Roy et al. 2002; Sá et al. 2003; Chuvieco et al. 2005), NOAA-AVHRR (Barbosa et al. 1998; Roy et al. 1999; Fuller and Fulk 2001; Nielsen et al. 2002), SPOT VEGETATION (Stroppiana et al. 2002; Silva et al. 2004), Landsat (Conese and Bonora 2005). Miettinen (2007) who have successfully mapped burned forest area in Kalimantan and Sumatera utilized multi-temporal MODIS, SPOT4, and SPOT 5 serta Landsat ETM+ data by applying index sensitive to vegetations behavior such as: NDVI, EVI (Huete et al. 2002), and GEMI (Pinty and Verstraete 1992). Suwarsono et al. (2009) has also successfully identified burned areas in Central Kalimantan, Indonesia, using NDVI method. On the other hand, Key and Benson (1999) employed Normalized Burn Ratio (NBR) index which is sensitive to water content level in plants to identify burned areas. Furthermore, Miller and Yool (2002), Cocke et al. (2005), and Escuín et al. (2008) have used NBR to determine the level of forest damage due to fire. Suwarsono et al. (2011) has also applied NBR method successfully using Landsat data to identify burned areas in Kalimantan, Indonesia. Although this vegetation index can be used to identify forest fire, it cannot be applied to identify logging activities. Therefore, more efficient and representative method is required to describe the two main causative phenomenon of forest degradation namely forest fire and logging.

A type of land cover classification techniques to identify degradation of satellite data is spectral mixture analysis (SMA). This technique can solve the problem arising in the visual classification and digital processing techniques. SMA method is an appropriate method for mapping degraded lands in the subpixel scale (Adams et al. 1995). This technique is able to detect changes in relatively small land area and provides physical value of the spectral satellite data. SMA techniques have also been applied by Souza et al. (2003) to map forest degradation due to selective logging and forest fires. Degradation analysis has been done using SMA technique in the Brazilian Amazon forest by using four fractions: the green vegetation fraction, canopy shadow fraction, soil fraction, and non-photosynthetic vegetation (NPV) fraction (Souza et al. 2003). Soil fraction obtained from SMA can sharpen spot detection and logging track (Souza and Barreto 2000). Asner et al. (2002) developed a gap fraction of green vegetation (GV) to estimate the fraction of forest canopy damage associated with selective logging, but the results tend to be overestimated. Furthermore, Souza et al. (2003) demonstrated the ability of NPV fraction to map selective logged forest. Souza et al. (2005) also integrated several fractions into Normalized Difference Fraction Index (NDFI) which gives better accuracy (94 %). Identification of forest degradation that occurs in a small area is very difficult to do, by merely relying on satellite data. Hence, complementary data in terms of field information or high-resolution spatial data are highly required.

The use of SMA and NDFI research method conducted by Souza et al. (2003, 2005) was applied in this study to indicate whether four fractions (GV, SHADE, SOIL, and NPV) and indices used in the study will be applied to identify forest degradation in West Kalimantan, Indonesia. Improvements were made in this study in applying the method to determine the threshold value of fraction and indices that correspond to forest degradation condition in Indonesia. The purpose of this study was (a) to identify the degraded forest area based on SMA approach, (b) to compare results of SMA approach, NDFI, with the widely used forest degradation index, the Normalized Burn Ratio (NBR) and the Normalized

Difference Vegetation Index (NDVI) in order to have enhanced detection of forest canopy damage caused by selective logging activities and associated forest fires in Kapuas Hulu and Sintang districts, West Kalimantan, Indonesia.

2 Datasets and methods

2.1 Study area

West Kalimantan province is one of provinces in Indonesia which lies on the equator. It has tropical climate with high temperature and high humidity. Most part of West

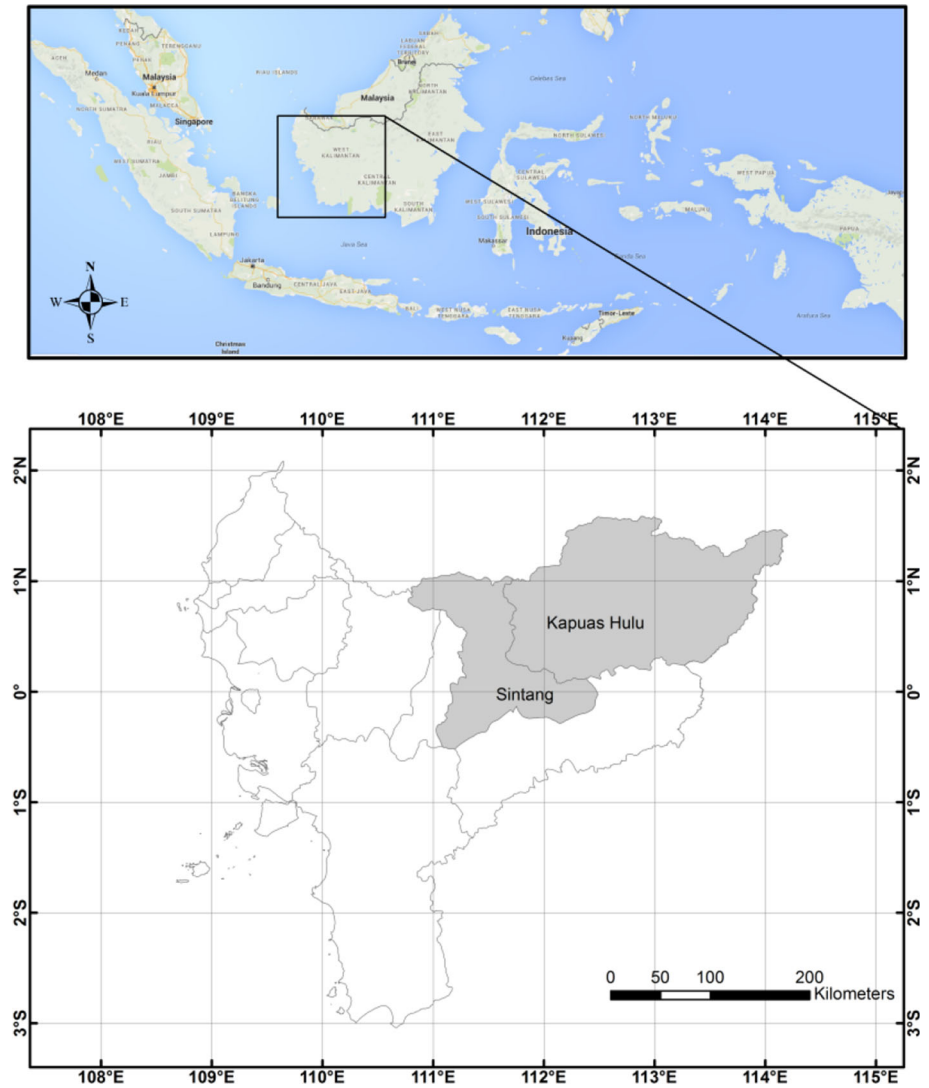


Fig. 1 Research area in Kapuas Hulu and Sintang districts, West Kalimantan

Kalimantan is lowland with a total area of approximately 146,807 km², covering 7.53 % of the total area of Indonesia. Forest predominantly covers approximately 42.42 % of West Kalimantan (BPS 2012). The research area is located in Kapuas Hulu and Sintang districts of West Kalimantan province (Fig. 1). Geographically Sintang district is located at 110°37'E–113°17'E and 1°03'S–1°16'S (Sintang district), while Kapuas Hulu is located at 111°26'E–113°59'E and 1°35'N–0°07'N.

Sixty percent (60 %) of watershed in West Kalimantan have experienced some kind of crisis as a result of exploitative actions by opening and developing watershed areas. The damage is due to activities such as illegal gold mining, logging, forest conversion to palm oil plantations, industrial activities, coastal erosion, destruction of mangroves, damaged to coastal areas, and coral reefs. The activity also has an impact on the occurrence of natural disasters along the Kapuas watershed such as: flood, landslides, and drought. The hydrology system of Kapuas River has the characteristics of wet months between 9 and 12 months with a fairly high rainfall between 3000 and 4500 mm/year. Kapuas watershed is essential because its upstream region is a water catchment area for West Kalimantan province and Kalimantan region as a whole (BPS 2012).

There were three classes of forest that was found by ground checking in the study area on October 9–14, 2012, as shown in Table 1.

2.2 Datasets

Satellite data used in this study are attained from Landsat-7 ETM+ path/row 120/60, acquisition date: July 23, 2006, May 7, 2007, August 5, 2008, July 31, 2009, and continued with SPOT-4 data acquired on July 31, 2009, May 16, 2012, and October 15, 2012. Such data were acquired from satellite ground station of Indonesian National Institute of Aeronautics and Space (LAPAN) in Pare–Pare, South Sulawesi. The study area also considers the topography data from DEM SRTM 90 m, and forest map area obtained from General Directorate of Planology, Ministry of Forestry in 2009. The location of protected forest and production forest in the upstream region was determined by the forest map area with relatively higher topography compared to the surrounding area. The area requires close supervision on forest conditions to prevent the expansion of plantation areas, particularly in the areas of production forest that is closely located to the area for other uses. For wider scale mapping, i.e., the West Kalimantan province, Landsat mosaic imagery and free cloud masking from 2000 to 2009 were used. The data were obtained from Indonesian National Carbon Accounting System Space activities conducted by LAPAN.

Table 1 Characterization of the forest degradation classes defined in the field scale

Forest degradation classes	Field description
Intact forest (IN)	Undisturbed forest
Managed logging (ML)	Planned selective logging where a tree inventory is conducted, there are roads in the area
Logged and burned (LB)	Either non-mechanized or conventionally logged forest that have subsequently been damaged by forest fire

2.3 Methods

2.3.1 Preprocessing remotely sensed imagery

The initial preprocessing of satellite data was performed empirically, which consists of: radiometric correction, geometric correction, and then the cloud masking. In the geometric correction, we used an image that already geometric corrected as the reference of uncorrected images. We performed the rectification using linear polynomial transformation and put 16 of ground control points in the image with the root-mean-square errors less than 0.5 pixel.

In this study, terrain correction step was conducted based on C-correction algorithm (Wu et al. 2004) as follows:

$$LH = LT(\cos(sz) + c)/(\cos(i) + c) \tag{1}$$

where LH is corrected radiance in flat surface, LT is uncorrected radiance in sloping surface, sz is sun zenith angle, *i* is the norm angle of the surface to the sun, and *c* is the coefficient value from ratio of *b* to *a* taken from the equation of $LT = a \cos(i) + b$.

We also performed the radiometric correction to avoid radiometric errors or distortions due to the sun’s azimuth and elevation, atmospheric conditions such as fog or aerosols and sensor’s response which influence the observed energy. In this study, we performed the radiometric correction due to sensor sensitivity and also due to sun angle which can be done in two steps, i.e., (1) converting the digital values into spectral radiance value, (2) converting the spectral radiance value into reflectance value. This is called as top-of-atmosphere (TOA) reflectance value (Edwards1999; Chander et al. 2009). The formula can be seen as follows:

$$L = (DN/A) + B \tag{2}$$

$$\rho = \frac{\pi d^2 L}{ESUN \cos \theta} \tag{3}$$

where *L* is spectral radiance (W/m²/sr/μm), DN is digital number of satellite data, *A* is the absolute calibration gain value, and *B* is absolute calibration offset value.

In this study, cloud and smoke haze masking was done by applied the threshold of the green and SWIR reflectants of the SPOT-4 taken from Sofan et al. 2011. They found that the green channel was good to separate the cloud from the others object such as cloud shadows, non-vegetation, and vegetation area, while the ad SWIR channel was good to represent the cloud shadow area. The threshold value of green and SWIR reflectance of thin to thick cloud and cloud shadow can be seen in Table 2.

Table 2 Threshold of thin to thick cloud and cloud shadow masking from SPOT-4 data (Sofan et al. 2011)

SPOT-4	Thin cloud/smoke haze		Thick cloud		Cloud shadow	
	Minimum	Maximum	Minimum	Maximum	Minimum	Maximum
Green channel	> 0.13	>0.19	>0.20	>0.26		
SWIR channel					<0.07	<0.09

2.3.2 Endmember extraction

Endmember is a spectral value representing the material in the earth’s surface. The endmembers can be received from the spectral images values and collections of laboratory and/or field spectra. The endmembers generated from images are called as image endmembers (Adams and Gillespie 2006). In this study, we generated the endmember from Landsat-7 and SPOT-4 satellite data images based on principle component analysis (PCA) method. There are four kinds of endmember images extracted in this study, i.e., GV, soil (SOIL), shadow (SHADE), and NPV.

2.3.3 Spectral mixture analysis (SMA)

In this study, each of satellite image was extracted into four fractions of GV, NPV, SOIL, and SHADE. The SMA model assumes that the image spectra are generated by a linear combination of n pure spectra. For example, a pixel is made up of 35 % of material A, 15 % of material B, and 50 % C material. The spectrum value of the pixel is the sum of weight of material A (0.35) against a spectrum of material A, weight of the material B (0.15) against material B spectrum, and weight of material C (0.50) against material C spectrum. Mathematically, image spectra can be formulated in Eqs. 4 and 5. The error in each image pixel can be calculated based on the root-mean-square error with Eq. 6 formula (Adams et al. 1993; Souza et al. 2005). The endmember fractions are then summed together for each pixel.

$$R_b = \sum_{i=1}^n F_i R_{i,b} + \varepsilon_b \tag{4}$$

$$\sum_{i=1}^n F_i = 1 \tag{5}$$

where n is the number of the samples. R_b is reflectance of band- b ; $R_{i,b}$ is reflectance value of endmember- i at band- b . F_i is fraction of endmember- i . ε_b is residual error of band- b .

$$\text{RMS} = \left[n^{-1} \sum_{b=1}^n \varepsilon_b \right]^{1/2} \tag{6}$$

where RMS is root-mean-square error, N is the number of samples, ε_b is residual error of channel- b .

Residual bands each pixel is calculated based on the difference between measured DN with DN modeled on each band. Residual of all bands are summed to give RMS error. The model is justified as a good model if: (a) residual band or RMS error is low, (b) fraction is not less than 0 or greater than 1. Pixels that have a high RMS error and fractions <0 or >1 indicate compositional variations that are not modeled on the scene (Adams et al. 1993).

2.4 Normalized Difference Fraction Index (NDFI)

Souza et al. (2005) developed a Normalized Difference Fraction Index which can be formulated from several fractions of SMA models. This is aimed to obtain sharper degradation signal due to selective logging and forest fire. The NDFI can be formulated using Eqs. 7 and 8.

$$\text{NDFI} = \frac{\text{GV}_{\text{shade}} - (\text{NPV} + \text{SOIL})}{\text{GV}_{\text{shade}} + \text{NPV} + \text{SOIL}} \quad (7)$$

where GV_{shade} is a fraction of GV normalized with SHADE fraction, given by,

$$\text{GV}_{\text{shade}} = \frac{\text{GV}}{100 - \text{SHADE}} \quad (8)$$

NDFI value ranges between -1 and 1 . NDFI of natural forests shows a high value (1) due to the combination of high GV and SHADE (high GV and high SHADE) and a low value of NPV and SOIL. Degraded forest will have increased value of NPV and SOIL fraction, lowering down NDFI value in comparison with that of natural forest.

2.5 Normalized Burn Ratio (NBR) and Normalized Difference Vegetation Index (NDVI)

Other than NDFI index resulting from SMA fraction, this study also used the burned area index, which is Normalized Burn Ratio and Normalized Difference Vegetation Index. NBR index can be obtained by calculating NIR and SWIR channel reflectance presented in Eq. 9 (Key and Benson 1999). NDVI can be obtained by calculating NIR and RED channel reflectance presented in Eq. 10 (Heiskanen 2006; Jensen 1986; Rouse et al. 1973).

$$\text{NBR} = (\rho_{\text{nir}} - \rho_{\text{swir}}) / (\rho_{\text{nir}} + \rho_{\text{swir}}) \quad (9)$$

$$\text{NDVI} = (\rho_{\text{nir}} - \rho_{\text{red}}) / (\rho_{\text{nir}} + \rho_{\text{red}}) \quad (10)$$

where NBR is Normalized Burn Ratio, NDVI is Normalized Difference Vegetation Index, ρ_{nir} is NIR channel reflectance, ρ_{swir} is SWIR channel reflectance, and ρ_{red} is RED channel reflectance.

2.6 Statistical analysis

Tukey's test was performed to evaluate whether natural forests and degraded forests can be separated at 95 % confidence level ($P > 0.05$). Tukey's test known as Tukey's honest significant difference test (HSD) is shown in Eq. 11. The test compares the means of every treatment to the means of every other treatment, that is applies simultaneously to the set of all pairwise comparisons (Hogg and Craig 1994; Ott 1992).

$$\text{Test: } H_0 : \mu_i = \mu_j, \quad H_0 : \mu_i \neq \mu_j$$

where the subscripts i and j represent two different populations.

$$\text{Test statistic: HSD} = q \sqrt{\frac{\text{MSE}}{n}} \quad (11)$$

$$\text{Decision: Reject } H_0 \text{ if } |\mu_i - \mu_j| > \text{HSD} \quad (12)$$

where q is the value from attached studentized range table, MSE is the mean-square error from ANOVA table, n is the number of replicates per treatment.

In this research, we have a limitation for the ground survey due to the difficulty to access the road to the expected location. Thus, it can affect the accuracy of the calculation results. In the future research, it can be developed and carried out detailed observations in order to obtain better accuracy.

3 Result and discussion

3.1 Multi-temporal analysis of imagery composite of Landsat-7 and SPOT-4

Figure 2 presents a composite colored image of RGB 542 Landsat-7 obtained multi-temporally in 2006, 2007, 2008, and 2009. The preserved forests or natural areas with high canopy density (dark green color) appeared in a good condition in 2006–2007. However, land opening started to occur in 2008, which expanded in 2009 (purple color). Subsequently in 2012, forest conditions in the study area can be seen from color composite image RGB 412 SPOT-4, and a significant change was evident from vegetation (green) becomes non-vegetation (pink color).

3.2 Endmember extraction from Landsat-7 and SPOT-4

Based on PCA analysis between bands 1–2, bands 1–3, and 3–4 bands of Landsat imagery, spectral endmember of GV, SOIL, SHADE, and NPV can be obtained. The endmember spectral profiles of all of SPOT bands presented in reflectance units are shown in Fig. 3a–e. The peak spectral reflectance of SOIL occurs at the fifth band (SWIR short-wave infrared: 1.55–1.75 μm) with mean and standard deviation values of 0.030 ± 0.0183 . The same spectral profile of SOIL is the NPV in which peak of reflectance presents in the SWIR band. The SWIR spectral reflectance value at NPV endmember is lower than that of SOIL. SWIR spectral reflectance on NPV endmember has mean \pm standard deviation of 0.1573 ± 0.0188 . The GV endmember has similar profile to the SHADE endmember, which has a peak reflectance at the fourth band (Near-Infrared: 0.75–0.90 μm). However, NIR reflectance on GV endmember has higher value than that of SHADE endmember. The average value of NIR spectral reflectance at GV endmember was 0.3709 ± 0.0206 , while the average value at SHADE endmember was 0.2258 ± 0.0067 .

The endmember spectral profiles of all of SPOT bands presented in reflectance units are shown in Fig. 3f–j. SOIL spectral has peak reflectance at XS-4 band (short-wave infrared or SWIR channel) with mean and standard deviation value of 0.3232 ± 0.008 . Same as SOIL spectral, the NPV spectral reaches its peak reflectance at SWIR channel, and the SWIR spectral reflectance values of the NPV are lower than that of the SOIL. SWIR spectral reflectance on NPV endmember has mean and standard deviation value of 0.2091 ± 0.0270 . GV endmember shows similar profile SHADE endmember, which has a peak reflectance at band XS-3 (Near-Infrared), but NIR reflectance of GV endmember has higher value than that of SHADE endmember. The mean value of NIR spectral reflectance at GV endmember was 0.3625 ± 0.0148 , while SHADE endmember was 0.2474 ± 0.0066 . Mean value analysis on each spectral endmember is subsequently used as a spectral reference in SMA-based classification process.

According to the result of Landsat and SPOT-4 data, the endmember of GV has a high value in NIR spectrum and low value in visible spectrum (blue, green, red). The live vegetation strongly reflects light in the near-infrared part of the spectrum, while the visible spectrum are efficiently absorbed by live vegetation. The SWIR spectrum is efficiently absorbed by water that content in the leaf. Different with GV, the senescent or dead vegetation (NPV) will reflect strongly in the SWIR spectrum due to less water content in the vegetation. Water is vital for many plant processes, in particular, photosynthesis. Generally, the vegetation of the same type with greater water content is more favorable and less prone to burn. Leaf water affects plant reflectance in the near-infrared and short-wave

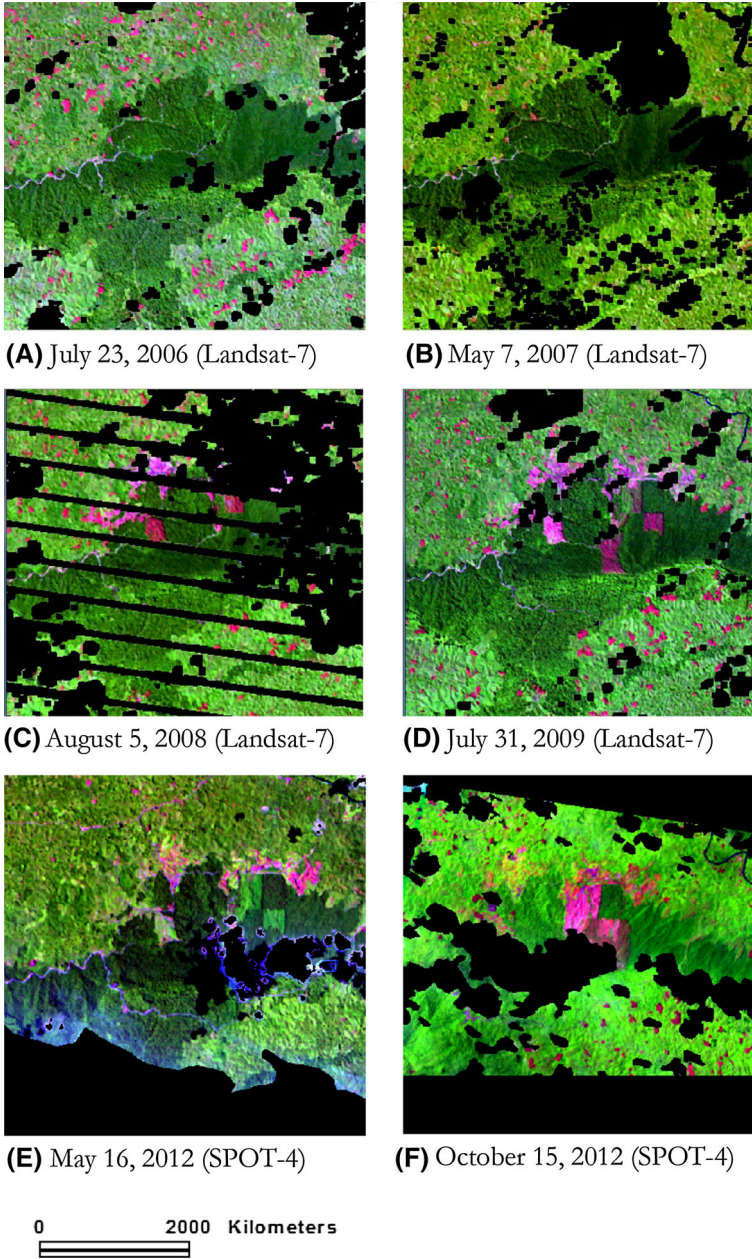


Fig. 2 542 RGB composite image of multi-temporal Landsat in 2006, 2007, 2008, 2009, and the 412 RGB composite image multi-temporal SPOT 4 in 2009 and 2012 in the study area

infrared regions of the spectrum. Water has maximum absorptions centered near 1.400 and 1.900 μm . Water features has centered spectral around 0.970 and 1.190 μm are pronounced and can be readily measured from hyper spectral sensors. That is way, the open

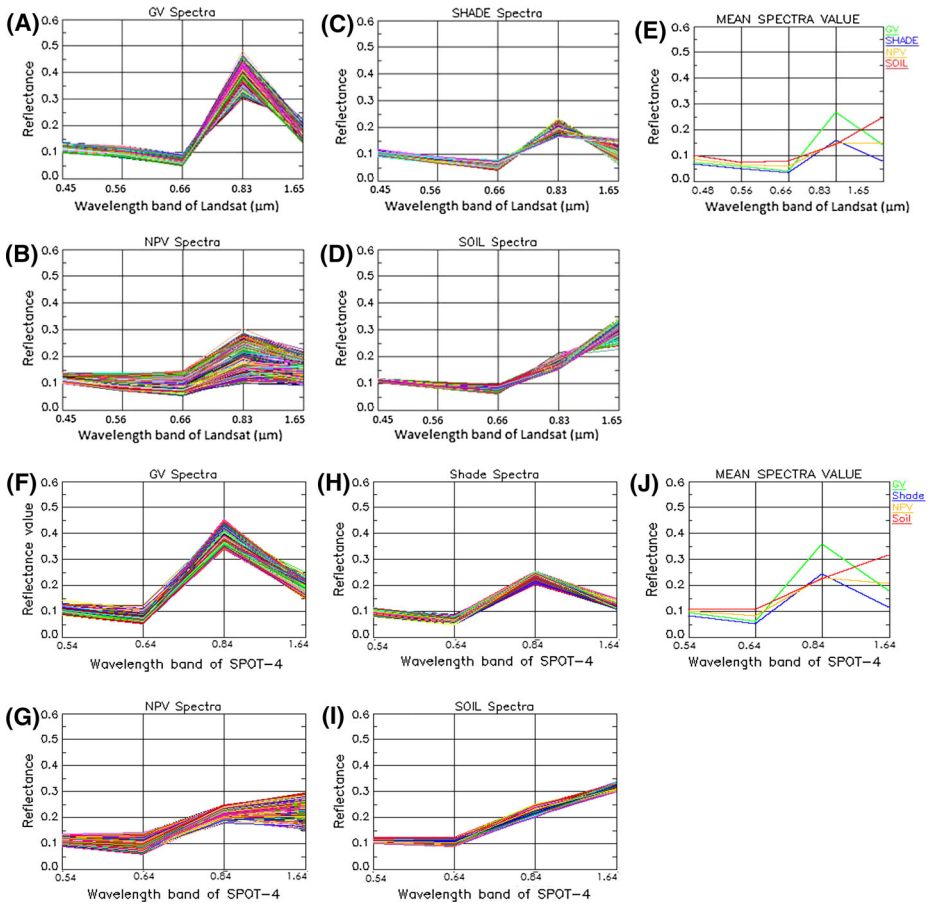


Fig. 3 Profile linkages between the reflectance and the wavelength bands of Landsat-7 and SPOT-4 on endmember analysis results with PCA method i.e., GV, NPV, SHADE, SOIL, and mean of spectra values

land that represented by SOIL endmember has a high reflectance in SWIR spectrum due to the lowest water content in the area.

3.3 Results of Spectral Mixture Analysis classification method on Landsat-7 and SPOT-4 data

Classification using SMA method is based on endmember spectral reference value of GV, NPV, SHADE, and SOIL in the study area. The results of endmember fraction ranges from 0 to 100 %, where the closer the value to 100 %, the higher the percentage of a fraction located at a pixel. An example is shown in Fig. 4, whereby each image of the four fractions dated July 23, 2006 which represents a natural forest condition, and dated July 31, 2009 which represents a degraded forest condition. GV image showed vegetation at their growth phase located outside the natural forest. GV fraction values outside the natural forest area in 2006 and 2009 were relatively similar (green color). Within the natural forests, vegetation generally has reached its maximum growth, so that GV fraction tends to be low

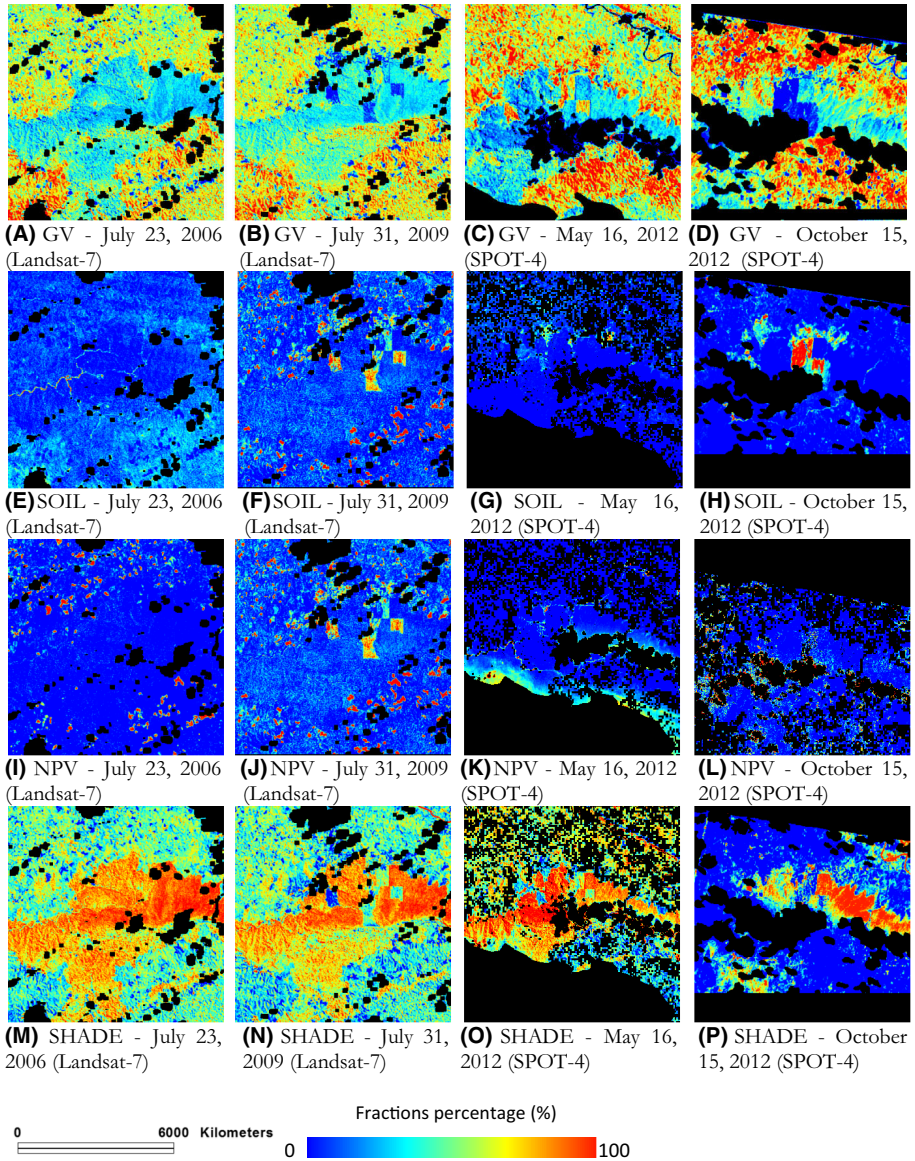


Fig. 4 Fraction images of GV, NPV, SOIL, and SHADE from Landsat data on July 23, 2006 and July 31, 2009 and from SPOT-4 data on May 16, 2012 and October 15, 2012 in the study area

(cyan–blue). In the natural forest areas, noticeable differences were evident in GV imagery in 2006 and 2009. In 2009, there were a few areas with lower GV (blue) than that in 2006. NPV image clearly showed that in 2009 there was additional NPV fraction area in natural forest marked with yellow and red coloration. In addition, SOIL fraction image in 2009 also showed increased percentage of SOIL fraction in natural forest sites, marked with yellow to red color. Meanwhile, through SHADE image it was observed that natural forests

generally have a high fraction values (red), but inside the forest, there were several visual difference. In 2009, there was a decrease in the SHADE fraction value (green to blue) compared to the previous condition in 2006.

Based on SPOT-4 data, endmember fractions image of GV, NPV, SHADE, and SOIL were acquired multi-temporally between period of May 16, 2012 and October 15, 2012, as also shown in Fig. 4. Range of SMA fraction image value is between 0 and 100. Non-vegetative land cover was observed at GV fraction image dated October 15, 2012 at low value (blue). Meanwhile, the NPV fraction image dated October 15, 2012 showed vegetation area at high NPV fraction values (red). This indicates that there is a decrease in vegetation canopy closure. SOIL fraction image in non-vegetation area demonstrated expansion of high fraction value (red) on October 15, 2012, indicating extension of ground objects area. Furthermore, in SHADE fraction image, part of the non-vegetative area shows a high SHADE fraction value (red). It indicates that the non-vegetative land has darker color soil than the surrounding soil, which may be due to slash and burn agriculture.

Based on RMS error analysis, results of SMA classification on Landsat-7 and SPOT-4 showed a relatively low error rates with maximum error of 0.05 % on each pixel. Based on its location, the maximum RMS error is 0.05 % on all Landsat-7 and SPOT-4 data are located in non-vegetative area. The error rate is relatively low, so it can be concluded that the fraction of GV, NPV, SOIL, and SHADE can be properly modeled with SMA.

3.4 Comparison of NDFI, NBR, and NDVI

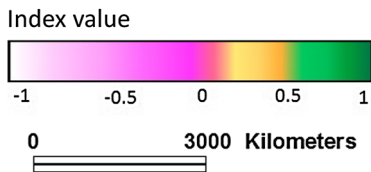
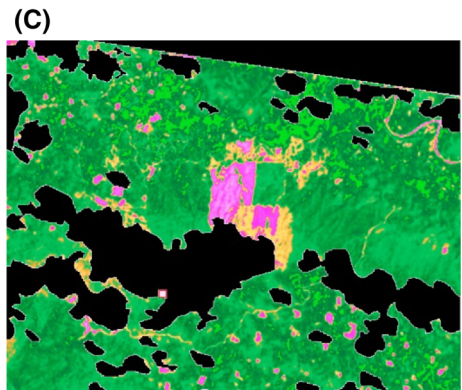
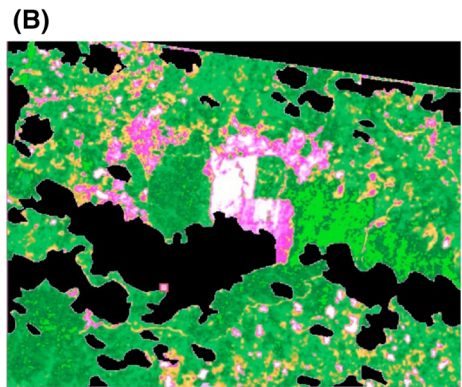
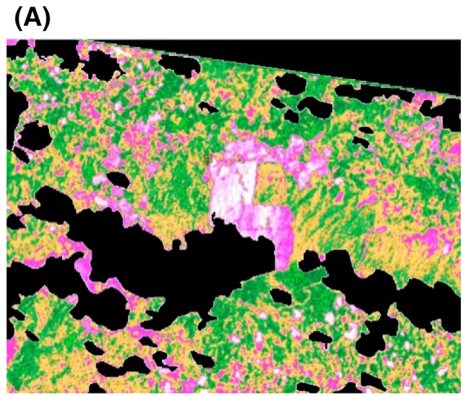
Other index like NBR and NDVI were also analyzed. Figure 5 shows the results of the analysis of all three indices, ranging between the values of -1 (blue) to 1 (red). The index value of -1 indicates high levels of forest degradation. The value of 1 indicates good forest condition with dense vegetation canopy cover. The NDFI image showed that the non-vegetation land has lower fractions value, while vegetation land area has high value. Meanwhile, from the NBR and NDVI image indices, it can be visually seen that the index value shows almost the same pattern: in non-vegetated territory, both indices showed a low value, whereas in vegetated land area, the indices showed high value. Based on the above description, visually and spatially, NDFI, NBR, and NDVI may represent forest conditions in both vegetated and non-vegetated area. Further statistical analysis is presented to assess the performance of these spectral indices.

3.5 Field survey

Spatially, the result of checking and determination of sampling points in field survey in Kapuas Hulu and Sintang districts can be seen in Fig. 6. During field survey conducted in October 10–15, 2012 in Kapuas Hulu and Sintang districts, several degraded forest were found, with damage due to logging and fires in the forest region. The degraded forest is located in Nanga Dangan, and Kapuas Hulu is part of protected forest area according to forest mapping by General Directorate of Planning in 2005. The forest in Kapuas Hulu district is located in highland area.

From field survey conducted in West Kalimantan province, three kinds of forests were found and used a reference in this study, namely: (a) forest with good condition, has not been exploited, and serves as protection of water system, flood prevention, and erosion control (Intact Forest); (b) regularly harvested forests and selected with good management (Managed Logging). Access road and heavy equipment are available in site; (c) Forests that are cut down and burned (Logged and Burned).

Fig. 5 Comparison of NDFI (a), NBR (b) and NDVI (c) analyzed from SPOT-4 data, October 15, 2012



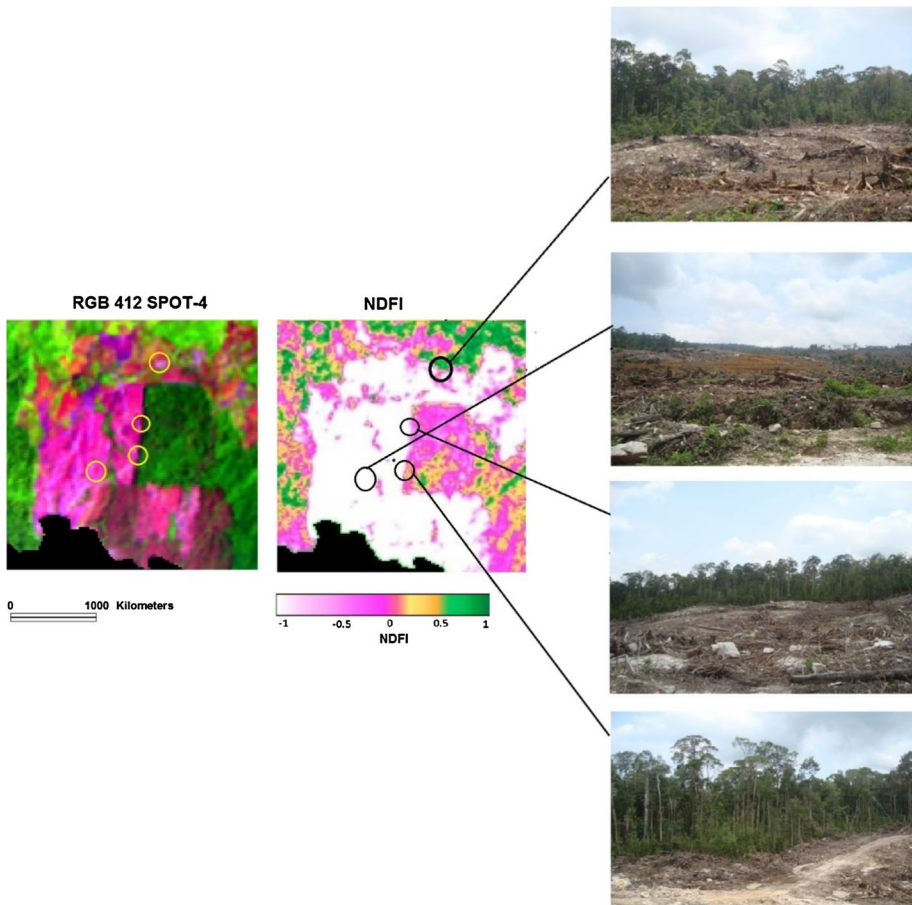


Fig. 6 NDFI image in Managed Logging area of Kapuas Hulu was analyzed from SPOT-4 image data acquired on October 15, 2012. The field photograph was taken on October 11, 2012. The *yellow and black circles* indicate the location of the ground survey

Figure 7 shows the control field at Managed Logging activity in the area at the Kapuas Hulu district, West Kalimantan. Based on RGB SPOT-4 image dated October 15, 2012, the vegetated areas close to the non-vegetation land generally is secondary forests where the tree diameters sized less than 20 cm and vegetation canopy are not densely closed. The NDFI index values in the region are low. Figure 7 shows the inspection results of Logged and Burned forest area in Sintang district, West Kalimantan. It can be seen from the photo, the logged, and burned area has dark colored soil, with some remaining pieces of tree roots. Based on RGB SPOT-4 image, the logged and burned area is shown in dark red color, with low the degradation index (NDFI) (blue).

3.6 Class separability, Tukey test, and accuracy results

The analysis of Tukey test was done to understand statistical difference between GV fraction, NPV, SHADE, SOIL, and also NDFI, NBR, and NDVI indices extracted within

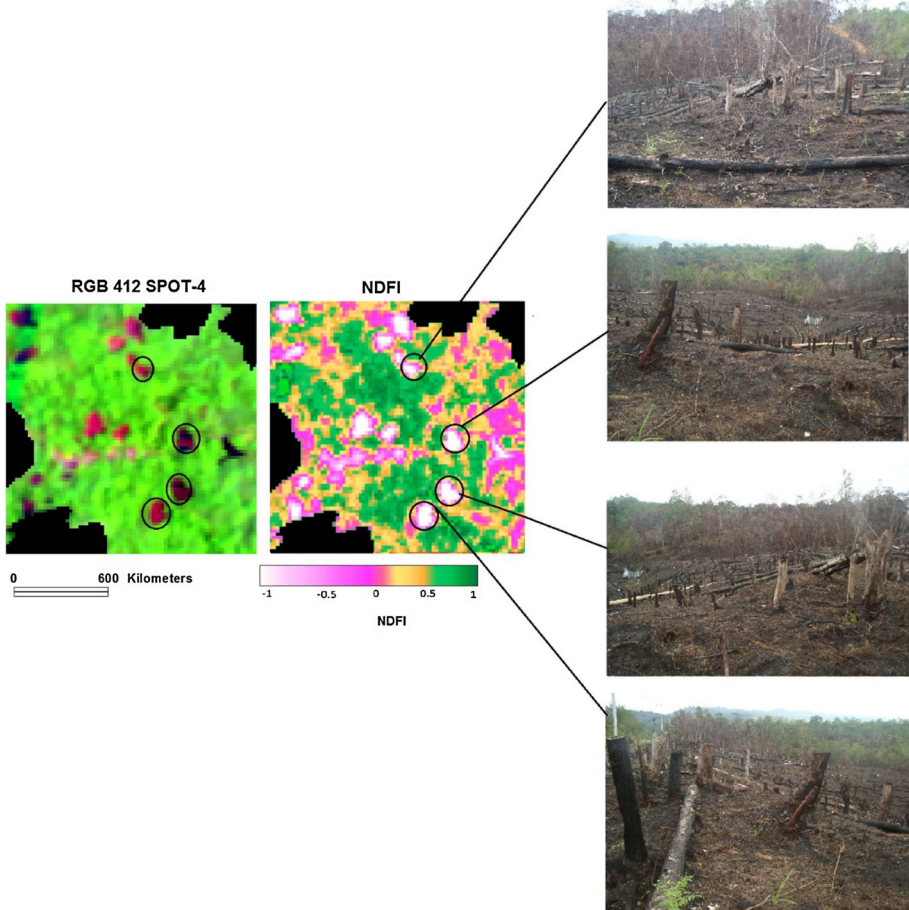


Fig. 7 NDFI image in logged and burned area of Sintang was analyzed from SPOT-4 image data acquired on October 15, 2012. The field photograph was taken on October 12, 2012. The *black circles* indicate the location of the ground survey

natural forest and degraded forest (IN and LB). Analysis of Tukey test at significance level (P) <0.05 showed that GV fraction, NPV, SOIL, SHADE and NDFI, NBR and NDVI index are statistically significant in Intact Forest and Logged and Burned forest. In Table 3, significant difference was marked on the average values with different letter sign (a, b, c). Tukey test results indicated that the hypothesis H_0 is rejected for all fractions and indices with significantly different value on Intact Forest and Logged and Burned forest. It means that they can be used to separate the Intact Forest and the degraded forest.

According to the statistical analysis, the composition of logged and burned forest consist of more than 50 % of SHADE and SOIL fractions, while the managing logged forest has high portion of NPV and GV fractions. We found that Intact Forest mostly consists of SHADE and GV fractions. Based on the fraction composition then, the NDFI has the lowest value (-0.96) in Logged and Burned forest and high values in Intact

Table 3 The mean and standard deviation (SD) values in intact forest and degraded forest

Fraction/index	LB		ML		IN		$ \mu_j - \mu_i $		HSD	$ \mu_j - \mu_i > \text{HSD}$ Decision ($P < 0.05$)	
	Mean	SD	Mean	SD	Mean	SD	LB-ML	LB-IN			
								ML-IN			
GV	1	5	30 ^b	8	26 ^c	7	0.041553	0.293276	0.251723	0.027071	Reject H_0
NPV	19 ^a	6	56 ^b	6	3 ^c	8	0.206862	0.462504	0.255641	0.055152	Reject H_0
SHADE	46 ^a	7	13 ^b	5	70 ^c	2	0.463825	0.690504	0.226679	0.020967	Reject H_0
SOIL	35 ^a	6	1 ^b	4	0 ^c	0	0.734081	0.745534	0.011453	0.03944	Reject H_0
NDFI	-0.96837 ^a	0.14056	-0.3149 ^b	0.281548	0.712028 ^c	0.256604	1.02695	1.680396	0.65347	0.072426	Reject H_0
NBR	-0.11163 ^a	0.063711	0.24744 ^b	0.019124	0.402691 ^c	0.01947	0.155248	0.514321	0.359073	0.012363	Reject H_0
NDVI	0.288196 ^a	0.058744	0.51948 ^b	0.025032	0.622207 ^c	0.017759	0.102726	0.33401	0.231284	0.011822	Reject H_0

The different sign letters indicate significant differences between classes of intact forest and degraded forest with the confidence level $P < 0.05$

Fig. 8 **a** Forest region map from Ministry of Forestry (2009) in West Kalimantan province. **b** Spatial distribution of NDFI image in West Kalimantan province from Landsat 2000–2009

Forest (0.72). The other indices, i.e., NBR show the negative value in Logged and Burned forest due to the lowest water content in the area. The key spectrum in NBR is SWIR spectrum that mostly absorbed by the water. In case of logged and burned area in which there is no water content, the SWIR is much reflected by the ground into the atmosphere and received by the satellite sensor. Meanwhile, the NDVI which represents the greenness level of vegetation indicated by high reflectant of NIR spectrum shows low NDVI in logged and burned area due to the low reflectant of NIR spectrum.

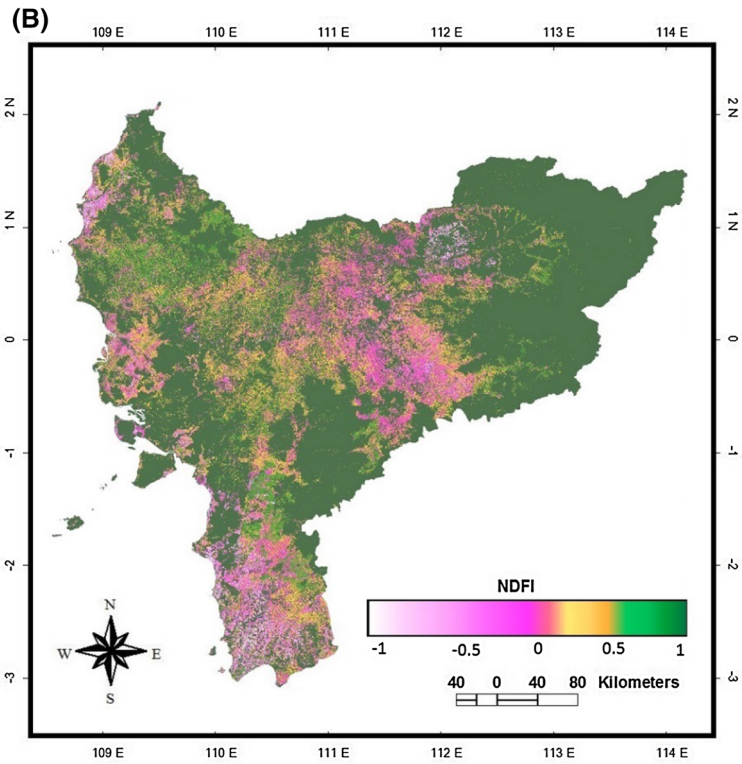
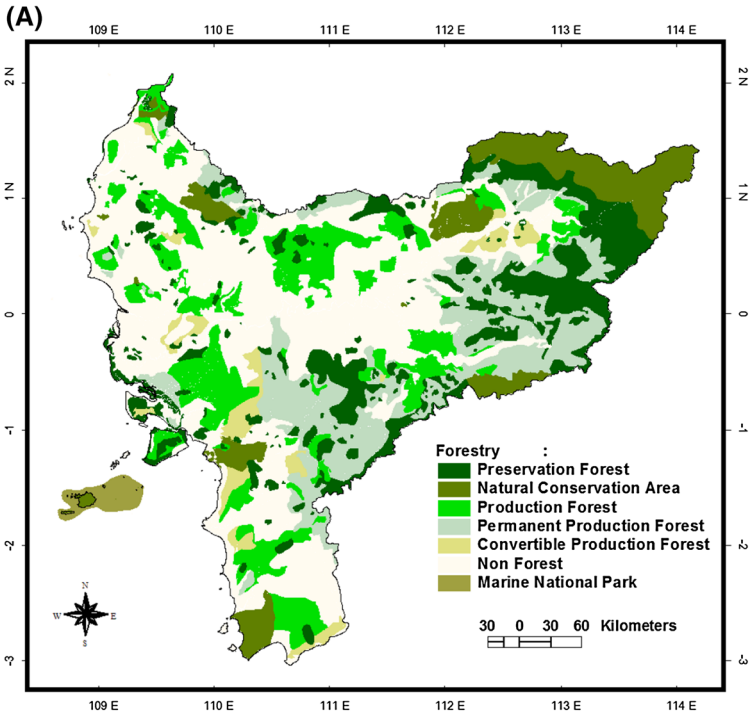
Based on Table 3, we found that the degraded forest in West of Kalimantan is in the range of negative and positive value of NDFI. This result is quite similar with the condition of degraded forest in Brazilian Amazon forest (Souza et al. (2005)) where they found the degradation forest classes in the range of positive value of NDFI. However, we also found the different for example the percentage of GV in LB area in our study area is differ with the Souza et al. 2005 result. In LB area, we got very few of GV fraction (average 1 %), while in Brazilian Amazon the GV fraction was around 25 % in LB area. Another facts that we found in LB area, the SOIL fraction was high (average 35 %) so when the forest logged and burned, there was no vegetation left and only left few NPV with the burned land cover. The lower negative of NDFI referred to the higher degraded intensity in the forest (Logged and Burned). The forest degradation could have the similar NDFI with the logged and burned forest, because they appeared same as the opened land without vegetation. For further research and to enhance the forest degradation caused by logged and burned activities, the deforestation sample area should be analyzed in this study.

The classification results of this research can be divided into two classes, namely: forest degradation (Managed logging forest, logged and burned forest) and non-forest degradation. Accuracy calculations are required to determine the accuracy of the classification results. The accuracy can be obtained by calculating Kappa, which is a matrix of contingency or confusion matrix. The calculation is done to test the significance of the classification results with the sample observations. The sampling was done by purposive sampling, with the purpose to obtain information related to whether or not the results of the classification. In these conditions, the location of the sample is determined by the ease of access road to the few locations that have been classified as experiencing changes due to forest degradation.

Table 4 shows the accuracy analysis that conducted toward the results of the degradation mapping of several indices, i.e., NDFI, NBR, and NDVI in forest areas Managed Logging (ML), Logged and Burned (LB), and Intact Forest (IN). NDFI results showed that

Table 4 Accuracy of forest types classification (managed logging/ML, logged and burned/LB, and intact forest/IN) from different indices (NDFI, NDFI-a, NBR, NDVI)

	NDFI	NBR	NDVI	Amount of data
ML	70.20	69.80	67.65	745
LB	94.91	66.10	74.58	118
IN	80.34	69.27	68.17	641



the index can provide better classification of forest ML, LB, and IN than other indices. Classification NDFI has the highest accuracy, with 95 % accuracy of forest-LB, 80 % of forests IN, and 70 % of ML.

3.7 Applications of NDFI for forest degradation mapping in province scale

Based on mosaic and cloud-free Landsat-7 data in the period of 2000–2009, NDFI method was applied to map degraded forest areas throughout the West Kalimantan province. Furthermore NDFI image was then integrated with forest maps obtained from the Ministry of Forestry in 2009, to determine the condition of forest types based on its NDFI value (Fig. 8).

Several forest types listed in the map according to the Ministry of Forestry in 2009 are: (1) Preservation forest whereby forest is preserved to maintain its protection functions principally as a life support system to adjust water cycle, prevent floods, control erosion, prevent seawater intrusion and maintain soil fertility; (2) Production forest, which refers to forest areas maintained to produce forest products for the benefit of public & industry consumptions, and exports; (3) Convertible production forest, the forest area reserved for the development of transmigration, settlements, agriculture and plantations; (4) Permanent production forest, a forest that can only be exploited by means of selective logging; (5) Natural conservation area, which is a forest area with certain characteristics, which located both in land and in water area, that have a protective function of life support systems, preserve diversity of plants and animals, and as support sustainable use of natural resources and its ecosystem.; (6) Non-forest area, i.e., an area of plantation, agriculture, and settlement. The forest map released by the Ministry of Forestry in 2009 showed that forest area in West Kalimantan reached about 60 % of the total area, or about 8.9 million ha. Non-forest area covers approximately 5.6 million ha or 38 %, and the rest are marine national parks and water body (rivers, lakes) 1 % each. In forest area, protected forest and production forest contribute 15 % each, while the limited production forest reaches 16 %, natural conservation area reaches of about 10 %, and convertible production forest area covers approximately 3 %.

We overlaid the NDFI imagery from Landsat with the forest map to investigate the mean value of NDFI for each types of forest used. The result of statistic values is presented in Table 5. We found that the preservation forest has the highest NDFI value (0.928 ± 0.231), while the lowest NDFI value is in the non-forest land (0.573 ± 0.466). The production forest has the lower value of NDFI compared with the other types of forest used. It related to the activities for forest consumption in production forest.

Table 5 NDFI statistic values (mean and SD) analyzed from Landsat-year period 2000–2009 in West Kalimantan per forest type

Forestry types	Mean	SD
Non-forest	0.573	0.466
Preservation forest	0.928	0.231
Production forest	0.696	0.448
Convertible production forest	0.804	0.348
Permanent production forest	0.863	0.298
Natural conservation area	0.863	0.397

4 Conclusions

The forest degradation was detected initially from 2008 until 2012 using Landsat 7 ETM + and SPOT-4 in Kapuas Hulu and Sintang districts, West Kalimantan. The spectral indices analysis (NDFI, NBR, NDVI) were tested and verified by ground survey data in 2012. The statistical test showed that those indices are statistically significant to distinguish the changes from intact forest to degraded forest. We found that NDFI has higher accuracy to classify the Logged and Burned area (95 %), Managed Logging area (70 %), and Intact Forest (80 %) than NBR or NDVI. Thus, it shows that the NDFI is significantly capable of detecting forest degradation in the tropical rainforest of West Kalimantan.

Furthermore, the application index NDFI with the value threshold has been applied using Landsat ETM + 7 to map each type of forest conditions either still undisturbed or degraded throughout the West Kalimantan province between 2000 and 2009. The use of NDFI methods is quite accurate in monitoring forest condition. Through remote sensing satellite data, updated information on latest forest condition in large area coverage can be obtained. Any indication of forest degradation which is mainly caused by fire and logging can be detected earlier without the need of directly visiting the area, and hence can pass the information to the responsible officials for rehabilitation and better forest management.

Acknowledgments This research was conducted in Remote Sensing Applications Center—LAPAN. Thanks go to Mr. Agus Hidayat, M.Sc. (The former Director of Remote Sensing Application Center, LAPAN) and Mr. Dedi Irawadi (The Director of Remote Sensing Application Center, LAPAN) who has supported this research. The author also would like to thanks to Indonesian National Carbon Accounting (INCAS) Project in Technology and Remote Sensing Data Center who support Landsat-7 data and also SPOT-4 data.

References

- Achard F, Hansen MC (2012) Global forest monitoring from earth observation. CRC Press, Boca Raton
- Adams JB, Smith MO, Gillespie AR (1993) Imaging spectroscopy: interpretation based on spectral mixture analysis. In: Pieters CM, Englert P (eds) Remote geochemical analysis: elements and mineralogical composition. Cambridge Univ. Press, New York, pp 145–166
- Adams JB, Sabol DE, Kapos V, Almeida Filho R, Robert D, Smith MO, Gillespie AR (1995) Classification of multispectral images based on fractions of endmembers: application to land-cover change in the Brazilian Amazon. *Remote Sens Environ* 52:137–154
- Adams JB, Gillespie AR (2006) Remote sensing of landscapes with spectral images: a physical modeling approach. Cambridge University Press, Cambridge
- Asner GP, Keller M, Pereira R Jr, Zweede JC (2002) Remote sensing of selective logging in Amazonia: assessing limitations based on detailed field observations, Landsat ETM + and textural analysis. *Remote Sens Environ* 80:83–496
- Bajracharya S (2008) Community carbon forestry: remote sensing of forest carbon and forest degradation in Nepal. Thesis, International Institute for Geo-Information Science and Earth Observation, Enschede
- Barbosa PM, Pereira JMC, Grégoire JM (1998) Compositing criteria for burned area assessment using multitemporal low resolution satellite data. *Remote Sens Environ* 65:38–49
- BPS (2012) Statistics of West Kalimantan
- Chander G, Markham BL, Helder DL (2009) Summary of current radiometric calibration coefficients for Landsat MSS, TM, ETM + , and EO-1 ALI sensors. *Remote Sens Environ* 113:893–903
- Chuvieco E, Ventura G, Pilar Martín M, Gomez I (2005) Assessment of multitemporal compositing techniques of MODIS and AVHRR images for burned land mapping. *Remote Sens Environ* 94:450–462
- Cochrane MA, Alencar A, Schulze M, Souza C Jr, Nepstad D, Lefebvre P, Davidson E (1999) Positive feedbacks in the fire dynamic of closed canopy tropical forest. *Science* 284:1832–1835
- Cocke AE, Fule PZ, Crouse JE (2005) Comparison of burn severity assessments using differenced normalized burn ratio and ground data. *Int J Wildl Fire* 14:189–198

- Conese C, Bonora L (2005) Burned land mapping from remote sensing imagery. Pecora 16 “global priorities in land remote sensing”, 23–27 Oct 2005, Sioux Falls, South Dakota
- Cox PM, Pearson D, Booth BB, Pierre F, Huntingford C, Jones CD, Luke CM (2013) Sensitivity of tropical carbon to climate change constrained by carbon dioxide variability. *Nature* 494:341–344. doi:[10.1038/nature11882](https://doi.org/10.1038/nature11882)
- Edwards AJ (1999) Application of satellite and airborne image data to coastal management (seventh computer-based learning module). UNESCO, Paris
- Escuin S, Navarro R, Fernandez P (2008) Fire severity assessment by using NBR (normalized burn ratio) and NDVI (Normalized Difference Vegetation Index) derived from LANDSAT TM/ETM images. *Int J Remote Sens* 29:1053–1073
- Fuller DO, Fulk M (2001) Burned area in Kalimantan, Indonesia mapped with NOAA-AVHRR and Landsat TM imagery. *Int J Remote Sens* 22:691–697
- Gerwing JJ (2002) Degradation of forests through logging and fire in the eastern Brazilian Amazon. *For Ecol Manag* 157(1):131–141
- Heiskanen J (2006) Estimating aboveground tree biomass and leaf area index in a mountain birch forest using ASTER satellite data. *Int J Remote Sens* 27(6):1135–1158
- Hogg RV, Craig AT (1994) Introduction to mathematical statistics. Prentice Hall PTR, Englewood Cliffs
- Huete A, Didan K, Miura T, Rodriguez EP, Gao X, Ferreira LG (2002) Overview of the radiometric and biophysical performance of the MODIS vegetation indices. *Remote Sens Environ* 83:195–213
- Jensen JR (1986) Introductory digital image processing. Prentice-Hall, Englewood Cliffs
- Johns J, Barreto P, Uhl C (1996) Logging damage in planned and unplanned logging operation and its implications for sustainable timber production in the eastern Amazon. *For Ecol Manag* 89:59–77
- Key CH, Benson NC (1999) Measuring and remote sensing of burn severity. In: Neuenschwander LF, Ryan KC (eds) Joint fire science conference and workshop, proceedings, vol II. University of Idaho and International Association of Wildland Fire
- Lanly J (2003) Deforestation and forest degradation factors. In: XII World Forestry
- Martín MP, Díaz-DeIgado R, Chuvieco E, Ventura G (2002) Burned land mapping using NOAA-AVHRR and TERRA-MODIS. In: Viegas (ed) Conference proceedings: forest fire research and wildland fire safety. Millpress, Rotterdam
- Miettinen J (2007) Burnt area mapping in insular Southeast Asia using medium resolution satellite imagery. Academic dissertation. Department of Forest Resource Management Faculty of Agriculture and Forestry University of Helsinki
- Miller JD, Yool SR (2002) Mapping forest post-fire canopy consumption in several overstory types using multi-temporal Landsat TM and ETM data. *Remote Sens Environ* 82:481–496
- Ministry of Forestry (2012) Forestry statistic. Water Catchment Management and Social Forestry Directory, Indonesia
- Ministry of Forestry (2013) Forestry statistic. Planology Directory, Indonesia
- Nepstad DC, Veríssimo JA, Alencar A, Nobre C, Lima E, Lefebvre P, Schlesinger P, Potter C, Moutinho P, Mendoza E, Cochrane M, Brooks V (1999) Large-scale impoverishment of Amazonian forests by logging and fire. *Int Wkly J Sci Nat* 398:504–508
- Nielsen TT, Mbow C, Kane R (2002) A statistical methodology for burned area estimation using multi-temporal AVHRR data. *Int J Remote Sens* 23:1181–1196
- Ott L (1992) An introduction to statistical methods and data analysis, 4th edn. California’ Duxbury Press, Belmont, 1051 pp
- Pinty B, Verstraete MM (1992) GEMI: a non-linear index to monitor global vegetation from satellites. *Vegetatio* 101:15–20
- Roberts DA, Batista GT, Pereira JLG, Walker EK, Nelson BW (1998) Change identification using multi-temporal Spectral Mixture Analysis: Applications in eastern Amazon. In: Luneetta RS, Elvidge CD (eds) Remote sensing change detection: environmental monitoring methods and applications, vol 9. Ann Arbor Press, Chelsea, pp 137–159
- Rouse JW, Hass RH, Schell JA, Deering DW (1973) Monitoring vegetation system in Great Plains with ERTS. In: Third earth resources technology satellite-1 symposium, 10–14 Dec 1973, Washington DC, NASA, pp 309–317
- Roy DP, Giglio L, Kendall JD, Justice CO (1999) Multi-temporal active-fire based burn scar detection algorithm. *Int J Remote Sens* 20:1031–1038
- Roy DP, Lewis PE, Justice CO (2002) Burned area mapping using multi-temporal moderate spatial resolution data—a bi-directional reflectance model-based expectation approach. *Remote Sensing and Environment* 83:263–286

- Sá ACL, Pereira JMC, Vasconcelos MJP, Silva JMN, Ribeiro N, Awasse A (2003) Assessing the feasibility of sub-pixel burned area mapping in miombo woodlands of Northern Mozambique using MODIS imagery. *Int J Remote Sens* 24:1783–1796
- Shimabukuro YE, Batista GT, Mello EMK, Moreira JC, Duarte V (1998) Using shade fraction image segmentation to evaluate deforestation in Landsat Thematic Mapper images of the Amazon Region. *Int J Remote Sens* 19(3):535–541
- Silva JMN, Cadima JFCL, Pereira JMC, Grégoire JM (2004) Assessing the feasibility of a global model for multitemporal burned area mapping using SPOT-VEGETATION data. *Int J Remote Sens* 25:4889–4913
- Sofan P, Zubaidah A, Vetrira Y, Yulianto F, Diah SKA (2011) Remote sensing application for mapping the burnt area. Internal report of National Institute of Aeronautics and Space (LAPAN) **(in Bahasa Indonesia)**
- Souza C, Barreto P (2000) An alternative approach for detecting and monitoring selectively logged forests in the Amazon. *Int J Remote Sens* 21:173–179
- Souza C Jr, Firestone L, Silva ML, Roberts DA (2003) Mapping forest degradation in the Eastern Amazon from SPOT 4 through spectral mixture models. *Remote Sens Environ* 87:494–506
- Souza C Jr, Roberts DA, Cochrane MA (2005) Combining spectral and spatial information to map canopy damage from selective logging and forest fires. *Remote Sens Environ* 98:329–343
- Stone TA, Lefebvre PA (1998) Using multi-temporal satellite data to evaluate selective logging in Para, Brazil. *Int J Remote Sens* 13:2517–2526
- Stroppiana D, Pinnock S, Pereira JMC, Grégoire JM (2002) Radiometric analysis of SPOT-VEGETATION images for burnt area detection in Northern Australia. *Remote Sens Environ* 82:21–37
- Suwarsono, Yulianto F, Parwati, Suprpto T (2009) The application of MODIS data for identifying burned area based on NDVI changes in Central Kalimantan Province. *J Remote Sens Digit Image Process* 6:54–64 **(in Bahasa Indonesia)**
- Suwarsono, Vetrira Y, Parwati, Khomarudin R (2011) Analysis of burned area in Central Kalimantan in 2009 using Normalized Burned Ratio from Landsat 7 SLC-off. In: *Proceeding of geospatial in development of region and city. Annual scientific conference. Indonesian Society for Remote Sensing (ISRS) (in Bahasa Indonesia)*
- Turner II BL, Moss RH, Skole DL (1993) Relating land use and global land-cover change: a proposal for an IGBP–HDP core project. IGBP report no. 24, HDP report no. 5. International Geosphere–Biosphere Programme, Stockholm
- Veríssimo A, Barreto P, Mattos M, Tarifa R, Uhl C (1992) Logging impacts and prospects for sustainable forest management in an old Amazon frontier: the case of Paragominas. *For Ecol Manag* 55:169–199
- Veríssimo A, Barreto P, Tarifa R, Uhl C (1995) Extraction of a high-value natural resource from Amazon: the case of mahogany. *For Ecol Manag* 72:39–60
- Verolme HJH, Moussa J (1999) Addressing the underlying causes of deforestation and forest degradation—case studies, analysis and policy recommendations. Biodiversity Action Network, Washington
- Wu X, Furby SL, Wallace JF (2004) An approach for terrain illumination correction. In: *The 12th Australian remote sensing and photogrammetry conference proceedings, Fremantle, WA*